Journal of Hydrology 614 (2022) 128532

Contents lists available at ScienceDirect

Journal of Hydrology

journal homepage: www.elsevier.com/locate/jhydrol

Research papers

Long-term trend of snow water equivalent in the Italian Alps

Nicola Colombo [a,b,*,1], Mauro Valt [c,d], Emanuele Romano [a], Franco Salerno [e], Danilo Godone [f,b], Paola Cianfarra [g], Michele Freppaz [h,b], Maurizio Maugeri [i], Nicolas Guyennon [a,1]

[a] Water Research Institute, National Research Council of Italy, Montelibretti, RM, Italy
[b] Research Center on Natural Risk in Mountain and Hilly Environments, University of Turin, Grugliasco, TO, Italy
[c] Avalanche Centre Arabba, ARPA-Veneto-DRST, Livinallongo del Col di Lana, BL, Italy
[d] AINEVA, Trento, Italy
[e] Institute of Polar Sciences, National Research Council of Italy, Venice, Italy
[f] Research Institute for Geo-Hydrological Protection, National Research Council of Italy, Turin, Italy
[g] Department of Earth, Environmental and Life Sciences, University of Genoa, Genoa, Italy
[h] Department of Agricultural, Forest and Food Sciences, University of Turin, Grugliasco, TO, Italy
[i] Department of Environmental Science and Policy, University of Milan, Milan, Italy

ARTICLE INFO

This manuscript was handled by Marco Borga, Editor-in-Chief, with the assistance of Francesco Avanzi, Associate Editor

Keywords:
Snow
Mountains
Standardised index
Teleconnection indices
Global warming
Drought

ABSTRACT

Snow stores a significant amount of water in mountain regions. The decrease of water storage in the snowpack can have relevant impacts on water supply for mountain and lowland areas that rely on snow melting. In this work, we modelled the Snow Water Equivalent (*SWE*) using daily snow depth (*HS*) data obtained from 19 historical *HS* measurement stations located in the southern European Alps (Italy). Then, we analysed the long-term (1930–2020) variability of the monthly Standardised *SWE* Index (*SSWEI*) and its links with climate change and large-scale atmospheric forcings (teleconnection indices). We found a marked variability in monthly *SSWEI*, with the lowermost values generally occurring in the last few decades (1991–2020), irrespective of elevation. In this recent period, highly negative values occurred at the snow season tails, mostly in spring. We found large-scale atmospheric patterns (North Atlantic Oscillation, Atlantic Multi-decadal Oscillation, and Artic Oscillation) and precipitation to be interconnected with *SSWEI* oscillations, although this relation changed after the 1980s, especially at low and medium elevations. This change occurred in correspondence of highly positive air temperature anomalies. In the last decades, we found increasing air temperature to be the main driver for the pronounced snow mass loss and persistent snow-drought conditions.

1. Introduction

The importance of snow as a seasonal water resource, threatened by climate change, is well-acknowledged (Immerzeel et al., 2010; Huss et al., 2017; Li et al., 2017). However, snow is not only a water resource, but it also plays a key role for sustaining ecological (e.g., Keller et al., 2005; Jonas et al., 2008; Freppaz et al., 2018) and socioeconomic (e.g., Rixen et al., 2011; Beniston, 2012) systems in mountains. Thus, observing snow-related variables, and their temporal variations, is pivotal for understanding the related processes and providing more reliable assessments of future changes (Beniston et al., 2018).

Among the different observed snow-related variables, Snow Water Equivalent (*SWE*) plays a crucial role. *SWE* is the mathematical product of snow depth (*HS*) and the snowpack bulk density (ρb), representing the equivalent amount of liquid water stored in the snowpack (Fierz et al., 2009). *SWE* is critical for flood and drought prediction (e.g., Jörg-Hess et al., 2015; Vionnet et al., 2020), hydropower management (e.g., Larue et al., 2017; Magnusson et al., 2020), ecological monitoring (e.g., Pauli et al., 2005; Huss et al., 2017), avalanche forecasting (e.g., Barfod et al., 2013; Hatchett et al., 2017), and mountain aquifer recharge (Lucianetti et al., 2017).

Despite the critical importance of *SWE*, fewer direct measurements are available for this variable than for *HS* (e.g., Sturm et al., 2010; Schöber et al., 2016), since manual and automatic measurements of ρb require complex and costly procedures (Egli et al., 2009; Kinar and Pomeroy, 2015). Therefore, consecutive, decades-long series of

* Corresponding author at: Water Research Institute, National Research Council of Italy, Montelibretti, RM, Italy.
E-mail address: nicola.colombo@irsa.cnr.it (N. Colombo).
[1] These authors equally contributed to the paper.

https://doi.org/10.1016/j.jhydrol.2022.128532
Received 25 July 2022; Received in revised form 20 September 2022; Accepted 29 September 2022
Available online 11 October 2022

measured *SWE* are uncommon and geographically scattered (Jonas et al., 2009; Avanzi et al., 2015). Indirect *SWE* measurements, such as through remote sensing techniques, can also be performed at various scales, although issues exist related to their spatial resolution, accuracy, and sensitivity (Dozier et al., 2016; Schattan et al., 2017; Steiner et al., 2018; Smyth et al., 2019). Finally, yet of primary importance for long-term studies, the available direct and indirect *SWE* measurements series generally cover few decades, which is short compared to several-decades-long *HS* data (Kinar and Pomeroy, 2015; Beniston et al., 2018).

Because of the reduced number of long-term datasets, there are only a few *SWE* trend studies, and most of them are focused on North America (e.g., Mote et al., 2018; Thakur et al., 2020; Elias et al., 2021). In the European Alps, for the period 1981–2010, large-scale gridded *SWE* datasets showed weak nonsignificant decreases, in contrast to the mostly negative *SWE* trends found in the Northern Hemisphere (Mudryk et al., 2015). Few studies analysed decades-long *SWE* trends in Switzerland, finding no trends in the Swiss Alps for the period 1975–1992 (Rohrer et al., 1994) and, differently, pointing out a general reduction of *SWE* in the last six decades (Marty et al., 2017). Only one study was performed in the Central Italian Alps (Bocchiola and Diolaiuti, 2010), finding that spring *SWE* decreased between 1965 and 2007.

Differently from *SWE*, several studies investigated multiple-decades-long *HS* trends in the European Alps, including Italy (Matiu et al., 2021, and references therein reported). *HS* data can be used to model *SWE*. Two main model types exist for this purpose: (i) empirical regression models (ERMs) and (ii) semiempirical models (SMs) (Egli et al., 2009; Winkler et al., 2021). ERMs derive *SWE* from *HS* and a combination of date, elevation, and regional parameters (e.g., Jonas et al., 2009; Pistocchi, 2016; Guyennon et al., 2019). Although capable to adequately model single *SWE* features (e.g., mean, peak, and seasonal *SWE*), ERMs are not suitable for calculating daily *SWE* from *HS* time series (Jonas et al., 2009; Winkler et al., 2021). Conversely, SMs are suitable for deriving *SWE* at daily resolution from continuous *HS* series, simulating individual snowpack layers, and taking advantage of the use of simple densification concepts (Winkler et al., 2021). However, compared to more complicated physically-based models (PBMs), they can only model ρb and *SWE*, while PBMs can also simulate snowpack features like energy fluxes, mass changes due to wind drift, grain types, etc. Unfortunately, PBMs require as input at least local temperature and precipitation information (De Michele et al., 2013) or climatological means (Hill et al., 2019), highly limiting their application in mountainous areas (Egli et al., 2009). Thus, in order to study long-term *SWE* changes using increasingly available decades-long *HS* data series, the use of SMs represents the most effective approach.

Long-term standardised *SWE* indices can be a useful tool for the analysis of long-term *SWE* changes and especially for investigating snow droughts (*SWE* deficits). The use of normalised indices, moving from absolute values to the frequency domain in terms of past estimated probability of occurrence (i.e., WMO, 2012), allows for a direct comparison of *SWE* time series collected at different locations and possibly affected by local and regional factors. In this framework, snow droughts remain relatively unexplored compared to other drought types (Huning and AghaKouchak, 2020), and only few studies have taken into consideration snow information for drought characterisation (e.g., Staudinger et al., 2014; Hatchett and McEvoy, 2018; Zhang et al., 2019), especially on the seasonal basis (Huning and AghaKouchak, 2020). This is particularly true for the Italian Alps (and European Alps, in general), where the temporal evolution of *SWE* deficits remains virtually unknown due to the lack of specific studies.

Further uncertainties exist on the relationships between snow variables and large-scale atmospheric forcings. Indeed, contrasting results have been reported regarding the behaviour of teleconnection indices and snow/precipitation dynamics in the Alps. For instance, in the European Alps, the North Atlantic Oscillation (NAO, Hurrell, 1995) was found to: (i) provide significant control upon snow variables and precipitation (Beniston 1997; Beniston and Jungo, 2002; López-Moreno et al., 2011); (ii) be only weakly and intermittently correlated to precipitation (Schmidli et al., 2002; Bartolini et al., 2009); (iii) play a minor role on snow cover and precipitation dynamics (Durand et al., 2009; Bartolini et al., 2010). Similar results were found for the Atlantic Multidecadal Oscillation (AMO, Kaplan et al., 1998; Zampieri et al., 2013; Nicolet et al., 2016, 2018; Brugnara and Maugeri, 2019) and the Artic Oscillation (AO, Li and Wang, 2003; Bartolini et al., 2009, 2010; Terzago et al., 2013).

Based on the previous considerations, in this study we aimed at unravelling the long-term variability in the water resources stored in the snowpack across the Italian Alps. To do this we: (i) retrieved daily *HS* measurements from 19 long-term weather stations distributed in the Italian alps, across an elevation range 750–2600 m a.s.l.; (ii) modelled daily *SWE* using the most recent and advanced SM available, ΔSNOW model (Winkler et al., 2021); (iii) calculated the monthly Standardised Snow Water Equivalent Index (*SSWEI*); (iv) investigated the elevational trends of *SSWEI*; (v) explored how *SSWEI* records are linked to climatic variables (large scale air temperature and precipitation, from reanalysis) and selected teleconnection indices (NAO, Winter NAO, AMO, and AO), in order to better understand the influence of climate change and large-scale atmospheric forcings on the regional *SSWEI* dynamics.

2. Data and methods

2.1. Study region

The Alps are the highest and most extensive mountain range system in Europe, stretching with their arc-shaped structure about 1,200 km across eight countries. Major rivers in Europe such as the Rhine, Rhone, Danube, and Po are fed by a network of tributaries originating in the Alps, whose significance for the regional water cycle is also expressed in the notion ‘‘water tower of Europe’’.

The Italian Alps roughly correspond to the southern European Alps, defined as the mountainous area south of the main Alpine watershed (Brugnara and Maugeri, 2019). In this region, the main climatic characteristic is the large influence of the Mediterranean Sea, which generally implies higher temperatures than in the northern slope, and higher orographically-driven precipitation due to the greater water content of the air (Isotta et al., 2014; Brugnara and Maugeri, 2019). The Alpine ecoregion in Italy is a well-defined combination of structural, climatic, and biogeographic features (Blasi et al., 2014). In our study, the geographical boundaries are those defined by the ISMSA/SOIUSA classification (International Standardized Mountain Subdivision of the Alps/ Suddivisione Orografica Internazionale Unificata del Sistema Alpino) (Marazzi, 2005) (Fig. 1).

2.2. Data series

The analysed dataset consists of continuous, daily measurements of snow depth (*HS*) retrieved from 19 manual and automatic stations located above 750 m a.s.l.; the largest part of the data derived from manual measurements. The stations are mainly located in flat, open areas, in the valley floors or near dams. All the stations cover the period encompassed between 1960 and 2020 (elevation range: 750–2600 m a.s.l.); among these stations, 15 cover also the previous 30-year period (1930–1959) (elevation range: 864–2200 m a.s.l.) (Table 1). In this way, the analysed stations are well-distributed over different elevations and climatic regions in the Italian South Western Alps, North Western Alps, and South Eastern Alps (following SOIUSA, Fig. 1). The data used in the present study were compiled by regional and provincial AINEVA avalanche services (Interregional Association for coordination and documentation of snow and avalanche problems), together with regional environmental protection agencies (ARPA Piemonte, ARPA Veneto), Regione Autonoma Valle d’Aosta, Meteotrentino, Italian Meteorological Society (SMI), hydropower companies (CVA S.p.A., Enel S.p.A.), and Ministry of Public Work (hydrological annals).

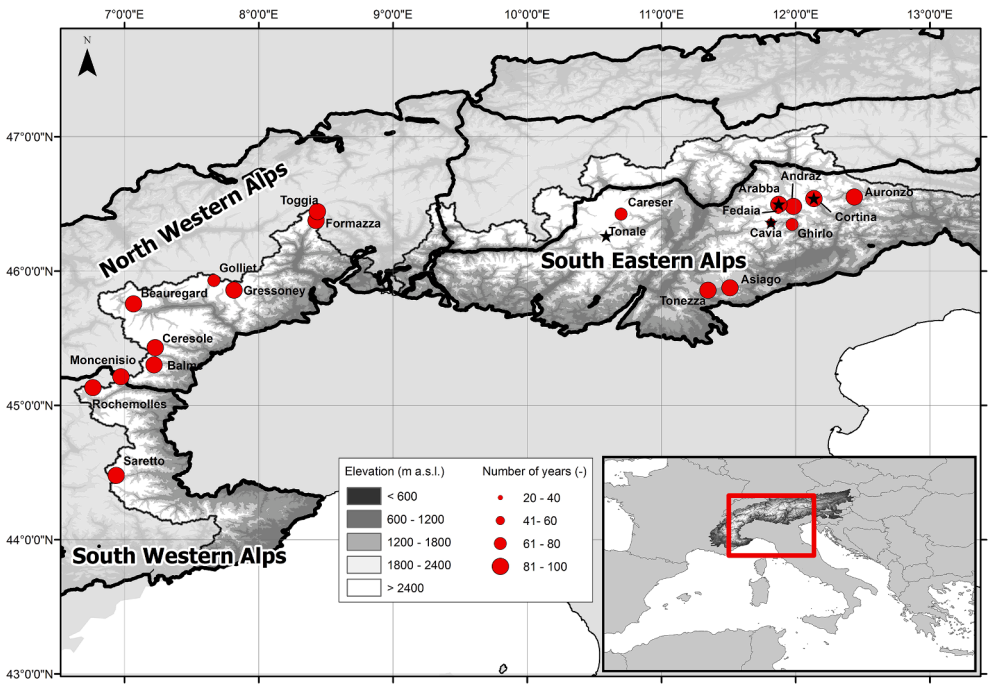

Fig. 1. Region of investigation showing the distribution of the *HS* stations. The thick black line delimits the sectors of the Italian Alps, according to the SOIUSA classification (Marazzi, 2005). The red circles identify the locations of the stations, while the dimension of the circles represents the time-series length; the name of each station is reported close to the respective red circle. The black stars refer to the stations used to validate the ΔSNOW model. The digital elevation model of the Italian Alpine chain is shown in grey scale within the Italian national border and shaded outside. More details regarding the stations are reported in Table 1. (For interpretation of the references to colour in this figure legend, the reader is referred to the web version of this article.)

Table 1
List of the stations used in this paper. *Stations used for model validation. **Stations used only for model validation. Mean and mean max monthly *SWE* refer to the time-frame 1960–2020, except for Cavia and Tonale (stations used only for model validation), whose values refer to their respective time-series length.

Name	Elevation (m a.s.l.)	Longitude (WGS84)	Latitude (WGS84)	Time-series length	Mean monthly *SWE* (mm)	Mean max monthly *SWE* (mm)	Missing (%)
Ghirlo	750	11°58′20.80″E	46°20′46.39″N	1953–2020	54	71	0.0
Auronzo	864	12°26′7.73″E	46°33′7.24″N	1922–2020	39	54	0.0
Tonezza	935	11°20′44.40″E	45°51′27.52″N	1927–2020	66	81	3.2
Asiago	1000	11°30′34.64″E	45°52′33.19″N	1920–2020	57	67	1.5
Cortina*	1250	12°8′8.35″E	46°32′25.70″N	1920–2020	91	127	3.0
Formazza	1280	8°25′34.61″E	46°22′36.80″N	1933–2020	170	257	0.6
Andraz	1440	11°58′56.66″E	46°28′55.61″N	1921–2020	98	153	0.0
Balme	1450	7°13′9.72″E	45°18′6.26″N	1928–2020	122	186	0.0
Saretto	1540	6°56′13.28″E	44°28′44.47″N	1924–2020	133	190	0.0
Ceresole	1579	7°13′40.31″E	45°25′49.14″N	1926–2020	134	193	0.0
Arabba*	1630	11°52′25.58″E	46°29′49.80″N	1929–2020	134	195	0.1
Beauregard	1772	7°3′58.69″E	45°45′21.44″N	1924–2020	179	257	1.4
Gressoney	1850	7°48′52.33″E	45°51′31.56″N	1939–2020	157	292	0.5
Tonale**	1880	10°35′16.36″E	46°15′38.93″N	1988–2020	196	318	0.0
Rochemolles	1929	6°45′47.88″E	45°7′58.07″N	1925–2020	198	363	0.9
Moncenisio	2000	6°58′19.99″E	45°12′46.83″N	1939–2020	186	330	0.8
Fedaia	2050	11°52′12.91″E	46°27′32.62″N	1964–2020	230	384	0.2
Cavia**	2100	11°48′57.87″E	46°21′36.33″N	1967–2020	241	386	0.0
Toggia	2200	8°26′10.64″E	46°26′33.76″N	1932–2020	456	751	0.8
Golliet	2526	7°39′54.16″E	45°55′45.76″N	1947–2020	343	543	0.1
Careser	2600	10°41′55.99″E	46°25′25.11″N	1936–2016	324	489	0.4

Data quality was firstly assessed by AINEVA, which replaced below zero *HS* values and outliers with missing values. In addition, we further carefully checked the series in order to remove possible recording errors by applying a temporal consistency check to the *HS* station records. We screened the series for jumps>40 cm (up), 30 cm (up, preceded by a zero), and 20 cm (down) on two consecutive days; we checked manually all the resulting values and replaced the recording errors with missing values. Several hundred events were visually checked, and only few dozens were actually recording errors. Globally, missing values affected approximately only 1 % of the entire dataset, with a maximum value of 3.2 % for single series (Table 1). We filled the data gaps shorter than 3 days by linear regression, while longer data gaps were left unchanged. Since the annual cycle of the Snow Water Equivalent (*SWE*) is shaped by snow accumulation and melting, we decided to entirely exclude from the analyses the snow seasons presenting data gaps at the beginning (i.e., November, December, January). Differently, in case of data gaps not affecting the beginning of the snow season, we excluded periods only after the missing values (until the end of the snow season). This step was necessary to prevent erroneous *SWE* simulations by not taking into account data gaps during the crucial period of the build-up of the seasonal snowpack (more details in "2.3 *SWE* modelling"), while avoiding the exclusion of entire snow seasons affected by some data gaps after the season beginning (i.e., melting period). Further details about the management of data gaps in the analyses are reported in section "2.6 Trend analysis".

Regarding the homogeneity of the data, a large effort was devoted by AINEVA to assess and eliminate inhomogeneities within the time series, resulting from several non-climatic factors that changed during the

historical investigated period (e.g., station relocations). For instance, in this work, we chose only stations that were not known to be affected by relevant station relocations or other affecting factors. Beyond this, applying appropriate homogeneity tests on long-term *HS* data is not straightforward and still subjected to large research efforts (e.g., Marcolini et al., 2017a; Marcolini et al., 2019), differently from temperature and precipitation records (Auer et al., 2007). For this reason, we performed the assessment of potential inhomogeneities only manually, thanks to the AINEVA effort.

For four stations (Cortina, Arabba, Tonale, and Cavia located at 1250, 1630, 1880, and 2100 m a.s.l., respectively), we retrieved measured *SWE* values, which we used to validate the ΔSNOW model (details in "2.3 *SWE* modelling"). Only two of them (Cortina and Arabba) are part of our long-term *HS* dataset, while the other two (Tonale and Cavia) are used only for validation purposes (Fig. 1, Table 1). These four stations were the only places across all our study area where biweekly or monthly *SWE* measurements were performed jointly with daily *HS* measurements. *SWE* was measured by hydropower companies and AINEVA between 1983 and 2020, using "layer" and "drill" methods. For the *SWE* "layer" calculation, the snow density (ρb) was measured, for each individuated homogeneous layer, by weighting a known volume of snow sampled horizontally. Valt et al. (2012) described the statistical procedure adopted for the calculation of the ρb and the integration of the layers having a thickness lower than the coring tube diameter. For the *SWE* "drill" calculation, a single vertical snow core was used (Berni and Giancanelli, 1966). Valt (2019) verified that the differences between the two methods were within 5 %.

2.3. SWE modelling

To model *SWE,* we used ΔSNOW, a new semiempirical multilayer model for simulating *SWE* and ρb from a regular time series of *HS* (Winkler et al., 2021). The model considers the change of *HS* as a proxy for the various processes altering ρb and *SWE*. ΔSNOW: (i) bases its (dry) snow densification function on Newtonian viscosity; (ii) provides a way to deal with small discrepancies between model and observation (*HS* measurement errors); (iii) takes into account unsteady compaction of underlying, older snow layers due to overburden snow loads; (iv) densifies snow layers from top to bottom during melting phases without automatically modelling mass loss due to runoff (more details in Winkler et al., 2021). The model does not take into account snow drift compaction and mass changes due to rain on snow, runoff during snowfalls, wind drift, little snowfalls, sublimation, and deposition. ΔSNOW can be used for estimating *SWE* in high-elevated areas with deep, long-lasting snowpacks as well as in valleys with shallow, ephemeral snowpacks.

In the ΔSNOW model, seven parameters can be calibrated: new snow density (ρ_0), maximum possible snow density (ρ_{max}), two viscosity parameters (η_0 and k), threshold deviation (τ), and two overburden parameters (c_{ov} and k_{ov}). To calibrate the model, Winkler et al. (2021) used snow observations of 67 winters from 14 stations, well distributed over different elevations and climatic regions of the European Alps. In addition, the authors used data from 71 independent winters from 15 stations for validation. In this work, we used the calibration proposed by Winkler et al. (2021) (Tab. S1). Indeed, the parameter setting suggested by the authors revealed to be optimal to model *SWE* from daily *HS* time series recorded at stations located in alpine areas, and with snow not older than an estimated 200 days. Regarding the latter, the mean duration of snow season (snow day, $HS > 1$ cm) was>200 days at five stations, all located above 2000 m a.s.l.; among these stations, we used only one, Toggia (2200 m a.s.l., Table 1), for the long-term trend analysis in the period 1930–2020 (details in "2.4 *SSWEI* and spatial/elevational patterns"). However, Cavia station, which was used to validate the model (details below), is located at 2100 m a.s.l. and had a mean snow season duration of ca. 205 days, therefore we also assessed the model's performance taking into account very long-lasting snowpacks.

We obtained 650 pairs of *HS* and *SWE* measurements from the stations used for ΔSNOW validation. Winkler et al. (2021) calibrated ΔSNOW using only those sites and years where and when the respective values of the daily *HS* record matched the values of *SWE* measurements. In our study, we used a threshold of ± 0.2 m as maximum *HS* discrepancy between daily value (at the stations) and measured *HS* (at the *SWE* measurement sites). This step was necessary since the measurement of *SWE* is a disruptive procedure, thus *SWE* and *HS* measurements could not always be taken exactly at the same place, which introduced uncertainty (cf., López-Moreno et al., 2020). The selected threshold allowed us to benefit of 501 observations for the validation. We assessed the performance of the *SWE* estimations through the analysis of the Pearson correlation (R), Mean Error (ME), Mean Absolute Error (MAE), and Root Mean Square Error (RMSE). ME, MAE, and RMSE are defined as follows:

$$ME = \frac{1}{n}\sum_{i=1}^{n} SWE_{obs} - SWE_{mod} \quad (1)$$

$$MAE = \frac{1}{n}\sum_{i=1}^{n} |SWE_{obs} - SWE_{mod}| \quad (2)$$

$$RMSE = \sqrt{\frac{\sum_{i=1}^{n} (SWE_{obs} - SWE_{mod})^2}{n}} \quad (3)$$

where SWE_{obs} and SWE_{mod} are the observed and modelled *SWE*, respectively. ME, MAE, and RMSE are expressed in the same units of *SWE* (mm).

2.4. SSWEI and spatial/elevational patterns

For the calculation of standardised indices, at the monthly scale, a theoretical distribution and a reference baseline have to be chosen. We selected the 1961–1990 period as a reference baseline. Then, we tested the fit of two different distribution functions (Lognormal and Gamma, e.g., Jonas et al., 2009; Margulis et al., 2016) to the monthly mean simulated *SWE* data, using the negative log-likelihood criteria. We found the best fit for our data with the Gamma distribution. Therefore, we fitted a Gamma distribution for each month of the snow season, at each station. We defined the beginning and end of the snow season for each station as the first and last month having a minimum of 50 % of monthly mean $SWE > 0$ over the chosen baseline. Then, we calculated the Standardised *SWE* Index (*SSWEI*) according to Huning and AghaKouchak (2020).

To identify which correlations could be expected depending on horizontal and vertical distances between stations, we performed a spatial analysis on *SSWEI*. To do so, we carried out pairwise correlations (Pearson) between monthly *SSWEI* series from November to May. Only in this case, the analysis was performed for the 1960–2020 period in order to have more pairs of stations (all 19 stations). For all the following analyses (e.g., trends, periodicity, etc.), we used only the 15 stations with data in the period 1930–2020. For all analyses, we selected the stations with at least 90 % of the available months.

2.5. Climatic drivers and teleconnection indices

To study the influence of air temperature and precipitation on *SSWEI* variability, we used ERA5-Land, a reanalysis product derived by running the land component of ERA5 at increased resolution (9 km compared to 31 km) and at hourly time scale (Dee et al., 2011; Muñoz-Sabater et al., 2021). In our study, we used the simulations from 1950 to 2020, selecting all the grid points falling into the region of investigation (only the sectors where the stations were located), delimited by the SOUISA classification (Fig. 1). We produced monthly averages of mean daily temperature and cumulated total precipitation. Given the reduced

amount of grid points, we did not consider spatial or elevation differences, thus obtaining a single output for each month in the region of investigation. Then, we calculated the 2-m air temperature deviation from its long-term mean (1961–90) for each month, obtaining a region-wide, monthly air temperature anomaly *AT**. Finally, we calculated a monthly Standard Precipitation Index (*SPI*, McKee et al., 1993), considering a Gamma distribution calibrated on each month over the 1961–1990 baseline (cf. Romano et al., 2021).

We explored the possible relationships between *SSWEI* (as well as *AT** and *SPI*) and teleconnection patterns considering the following selected indices: North Atlantic Oscillation - NAO and Winter NAO - WNAO (Hurrell, 1995), Atlantic Multi-decadal Oscillation (AMO) (Kaplan et al., 1998), and Artic Oscillation (AO) (Li and Wang, 2003).

2.6. Trend analysis

We performed the trend analysis on *SSWEI* in the period 1930–2020 using the non-parametric Mann-Kendall (MK) test (Kendall, 1975), which is widely adopted to assess significant trends in hydro-meteorological time series (e.g., Valt and Cianfarra, 2010; Guyennon et al., 2013; Salerno et al., 2015). In this study, we applied the sequential MK test (seqMK) (Gerstengarbe and Werner, 1999) to monthly vectors. To monitor the overall non-stationarity of the time series, we analysed the progressive normalised Kendall's tau coefficient $\mu(\tau)$. We treated the few missing values in the series with a stationary assumption, thus preserving unchanged the values preceding the missing values. Finally, we performed the trend analysis also on monthly *AT** and *SPI*, in the period 1950–2020.

2.7. Analysis of periodicity

We explored the possible periodic components of the monthly *SSWEI* by means of a time–frequency wavelet analysis, adopting the Morlet transform. Unlike the classical Fourier transform, the wavelet transform allows a localisation of the signals in both frequency and time rather than in a simple frequency space. The mathematical bases of this technique are given by Grossmann and Morlet (1984) and a complete description is given by Torrence and Compo (1998). Moreover, we investigated the non-stationarity of the relationships between *SSWEI* and teleconnection indices using the wavelet coherence (WTC). The WTC is defined as the square of the cross-spectrum normalised by the individual power spectra. The WTC also allows finding high levels of significance even when the common power of the two series is low and thus it gives an accurate representation of the (normalised) covariance between the two time series (Torrence and Webster, 1999; Guyennon et al., 2014).

3. Results

3.1. Model validation

Modelled *SWE* had an overall R of 0.96, ME of 6.3 mm, MAE of 39.9 mm, and RMSE of 56.2 mm indicating a rather good performance in the representation of the *SWE* in our validation sites. Although in our case ΔSNOW performed moderately worse than in Winkler et al. (2021) (MAE = 21.9 mm, RMSE = 30.8 mm), we stress out the fact that we did not perform an ad-hoc calibration for our sites, considering the reduced number of *HS-SWE* pairs available in our study region. In addition, the elevation of our validation sites ranged from 1250 to 2100 m a.s.l., while in Winkler et al. (2021) the elevation range of the calibration/validation sites was between 590 and 1780 m a.s.l. Thus, we expected a rather worse performance of the model considering the higher elevations, and the longer snow seasons taken into consideration in our study. Indeed, we obtained the best modelling performance at the lowermost station (Cortina, 1250 m a.s.l., MAE = 30.6, RMSE = 37.8 mm) and the worst performance at the highermost one (Cavia, 2100 m a.s.l., MAE = 57.4, RMSE = 77.5 mm) (Fig. 2). Finally, Winkler et al. (2021) calibrated ΔSNOW using only those sites and years where and when the respective values of the daily *HS* record matched the values of the biweekly measurements. Differently, in our study, we selected a threshold for maximum *HS* discrepancy between daily value (at the stations) and measured *HS* (at the *SWE* measurement sites) of ± 0.2 m. Even though we used this threshold, our overall modelling performance was in line with the performances of other modelling studies performed in alpine areas, such as: Egli et al. (2009) (RMSE = 56 mm, SNOWPACK model), Jonas et al. (2009) (RMSE = 50.9–53.2 mm), Essery et al. (2013) (RMSE = 23–77 mm, various thermodynamic snow models), Sturm et al. (2010) (MAE = 51 mm, calibrated in Guyennon et al., 2019), Pistocchi (2016) (MAE = 50.6 mm, calibrated in Guyennon et al., 2019), and Guyennon et al. (2019) (MAE = 49.2 mm).

3.2. Elevation and spatial patterns of SSWEI

Mean monthly *SWE* values and snow cover duration showed increasing values according to elevation (Fig. 3a, Table 1), as expected. In particular, we found three main elevation clusters:

- Low elevation (5 stations): 750–1250 m a.s.l., mean *SWE*: 61 mm, mean max *SWE*: 80 mm, snow cover duration: January–March.
- Medium elevation (8 stations): 1251–1850 m a.s.l., mean *SWE*: 141 mm, mean max *SWE*: 215 mm, snow cover duration: December–April.
- High elevation (6 stations): >1850 m a.s.l., mean *SWE*: 290 mm, mean max *SWE*: 476 mm, snow cover duration: November–May.

In addition, the *SSWEI* correlation analysis showed that correlation coefficients decreased with both horizontal and vertical distance, although they remained high even for large distances (Fig. 3b). We found correlation coefficients equal to or higher than 0.7 for vertical distances of up to 600 m, with less than 200-km horizontal distance.

Considering these findings, we averaged the individual, station-based *SSWEI* values and performed the trend analysis on the 15 long-term stations (1930–2020), according to the three selected elevation bands.

3.3. Temporal variability and trends of SSWEI

The temporal variability of *SSWEI*, *SPI*, and *AT**, as a function of the three elevation bands, is shown in Fig. 4, whereas the results of the seqMK test applied to these variables are shown in Fig. 5.

In general, we found the lowermost monthly *SSWEI* values to occur in the period 1991–2020. Other interesting features of the *SSWEI* curves were the minima in the 1940s-1950s (March-May), and the maxima in the 1960s (November–January) and in the 1970s-1980s (February–May), irrespective of the elevation. All these minima and maxima were particularly evident in March (low elevation), March-April (medium elevation), and March–May (high elevation). For these months, the maximum *SSWEI* value was reached in the time lapse 1971–1990, which was then followed by a minimum around the early 1990s. After this minimum, a partial recovery or stabilisation was experienced at all elevation bands, although in general *SSWEI* remained negative until the end of the analysed time-frame.

The low *SSWEI* values of the last 30 years caused the results of the seqMK test to exhibit the lowermost $\mu(\tau)$ values in the 1991–2020 period for all months, across all the elevation bands. We found, however, a few exceptions, such as March (low elevation), April (medium elevation), and May (high elevation), which showed comparably negative values in the 1940s-1950s. Evident were also the high $\mu(\tau)$ values for *SSWEI* in almost all investigated months in the 1970s-1980s, across the three elevation bands. However, due to the high year-to-year variability of the *SSWEI* records, the corresponding $\mu(\tau)$ records reached a 95 % significance level only in a limited number of cases.

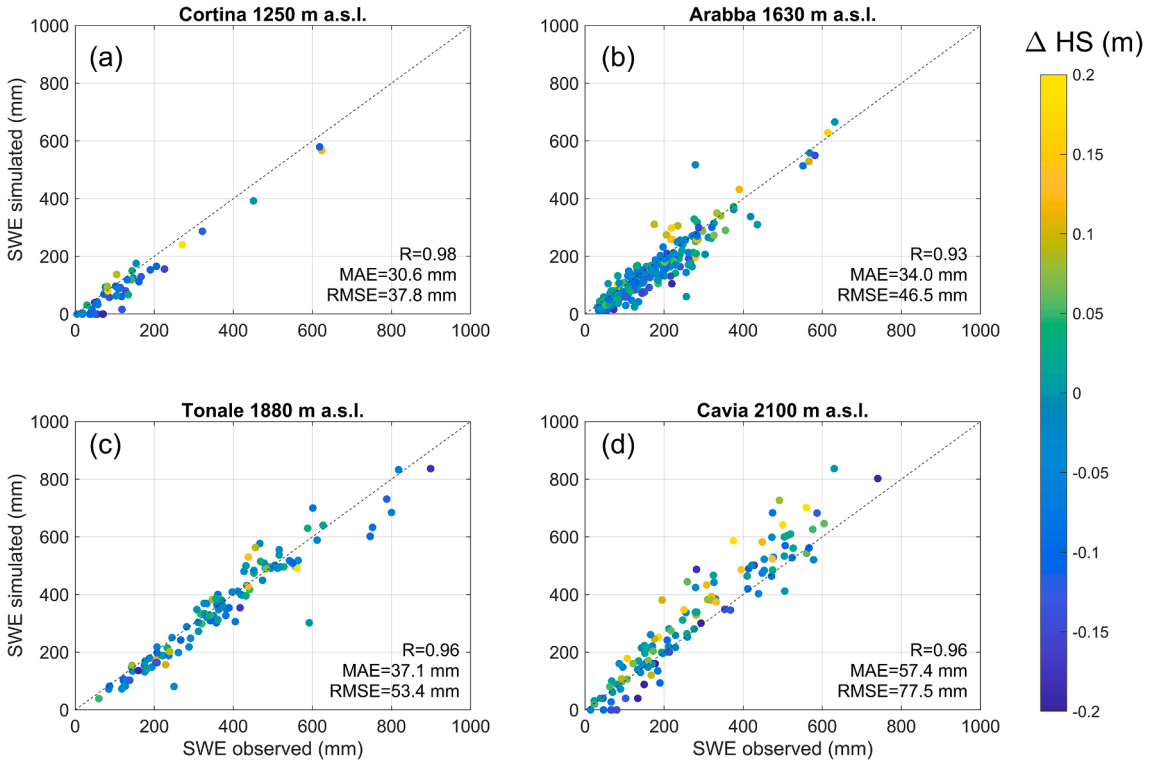

Fig. 2. ΔSNOW model validation at the stations (a) Cortina, (b) Arabba, (c) Tonale, and (d) Cavia. The colour scale refers to the discrepancy (Δ *HS*) between *HS* daily value at the stations and measured *HS* at the *SWE* measurement sites.

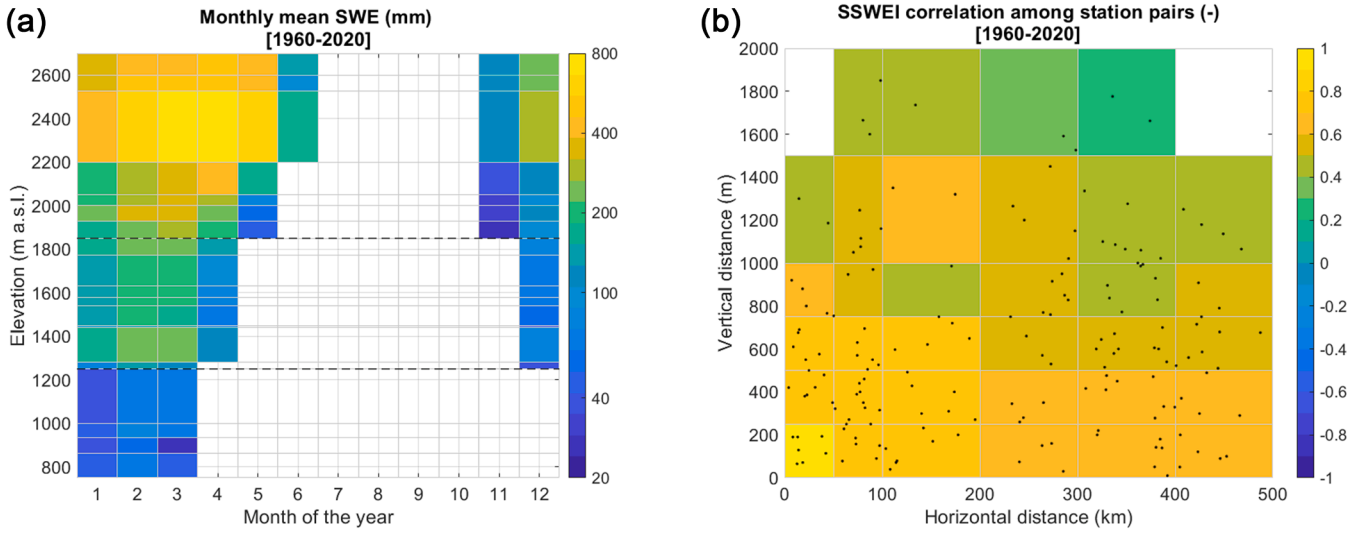

Fig. 3. (a) Overview of mean monthly *SWE* across the station elevation range (*SWE* values below 20 mm were not considered) and (b) summary of pairwise correlations (Pearson) between monthly *SSWEI* series from November to May (right). Data in both panels refer to all 19 stations (period: 1960–2020). The dashed lines in panel (a) highlight the identified three elevation thresholds.

The temporal behaviour of *SPI* showed a rather good agreement with the *SSWEI*'s one, across all elevation bands, indicating a general interconnection between precipitation and *SWE* dynamics. However, main divergence patterns between *SSWEI* and *SPI* emerged for specific months across different time frames: (i) in the 1960s, January (across all elevation bands) showed positive *SSWEI*, and negative *SPI* and *AT**; (ii) in the 1970s-1980s, April (at medium and high elevation) was characterised by positive *SSWEI*, and negative *SPI* and *AT**; (iii) in the period 1991–2020, March-April (medium elevation) and November-April-May (high elevation) exhibited decidedly negative *SSWEI*, from slightly negative to slightly positive *SPI*, and markedly positive *AT**; (iv) in the 2010s, January and February (at all elevations) and March (low elevation) evidenced negative *SSWEI*, from around zero to slightly positive *SPI*, and strongly positive *AT**. The divergences between *SSWEI* and *SPI* also emerged from the analysis of the μ(τ) records. Specifically: (i) in the 1960s, January and February (across all elevation bands) evidenced μ(τ) values generally above zero for *SSWEI*, and negative for *SPI* and *AT**; (ii) in the 1970s-1980s, April (medium and high elevation) exhibited μ(τ) values decidedly above zero for *SSWEI*, and negative for *SPI* and *AT**; (iii) in the period 1991–2020, November (high elevation), December

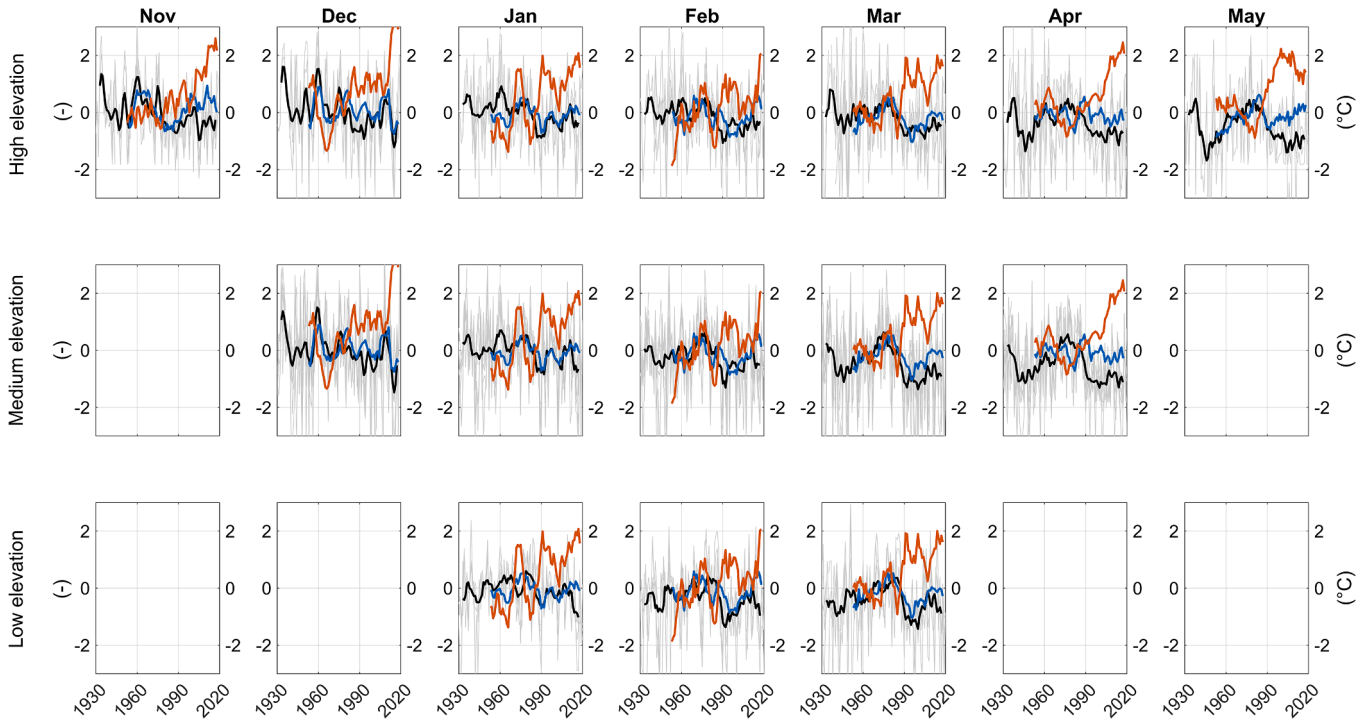

Fig. 4. *SSWEI* (grey), smoothed *SSWEI* (black), and *SPI* (blue) (primary Y axis); *AT** (red) (secondary Y axis). Monthly data are shown for low, medium and high elevation bands. We applied a 7-year moving average to *SSWEI*, *SPI*, and *AT** (smoothed data). *SPI* and *AT** are equal across elevation bands, and cover the period 1950–2020. (For interpretation of the references to colour in this figure legend, the reader is referred to the web version of this article.)

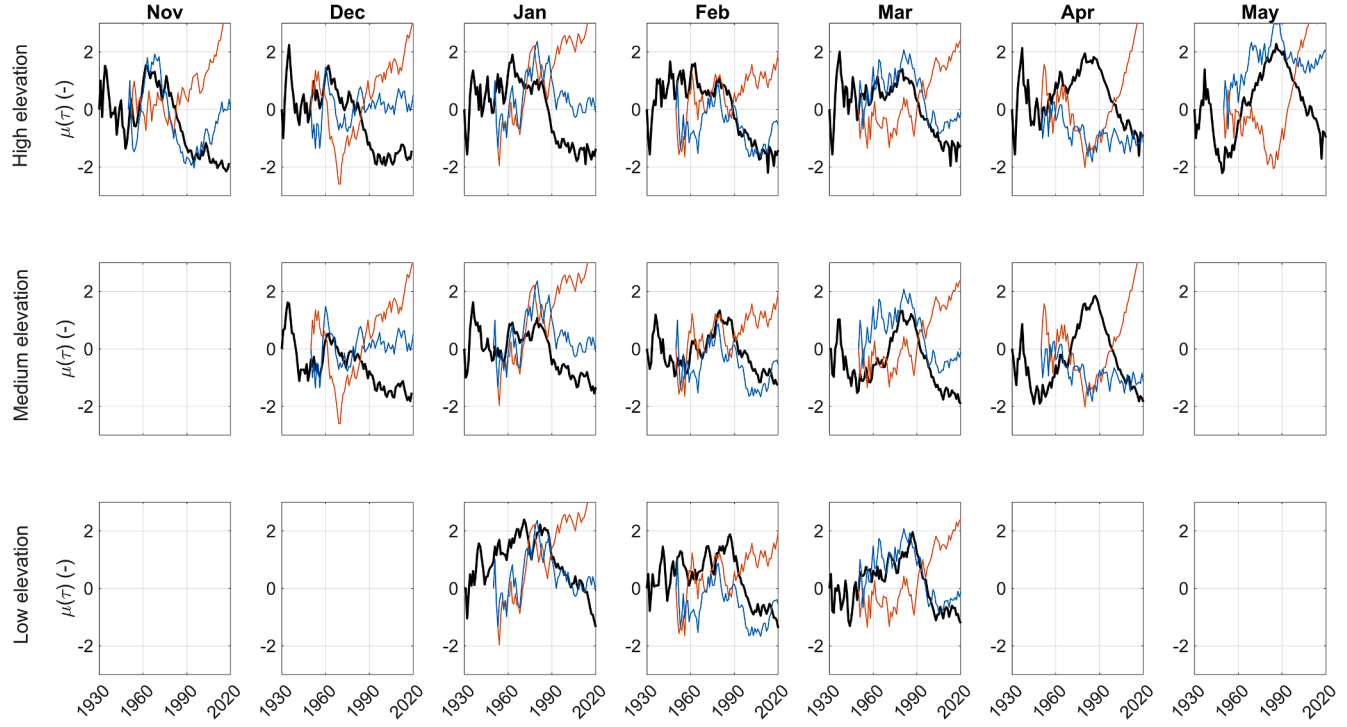

Fig. 5. Results of the seqMK test applied to monthly time scale for *SSWEI* (black), *SPI* (blue), and *AT** (red). Normalised Kendall's tau coefficient (μ(τ)) is reported; values below − 1.96 or above + 1.96 are significant at the 95 %. *SPI* and *AT** are equal across elevation bands, and cover the period 1950–2020. (For interpretation of the references to colour in this figure legend, the reader is referred to the web version of this article.)

(medium and high elevation), January (low, medium and high elevation), and March (medium and high elevation) showed μ(τ) values decidedly below zero for *SSWEI*, around zero (or slightly negative) for *SPI*, and markedly positive for *AT**. A clear divergence also emerged for May (high elevation), with a well negative μ(τ) for *SSWEI*, and positive values for *AT** μ(τ) and *SPI* μ(τ). Therefore, the agreement between *SSWEI* and *SPI* was lower mostly in the periods with strongest temperature anomaly and this was especially evident in the most recent period,

due to the very strong positive temperature trend in the last decades.

Figure S1 shows the wavelet transformation of the average monthly *SSWEI* time series of the three elevation ranges. This analysis did not give evidence of continuous periodic behaviour in any interval of the investigated period, with most of the power spectral density contained in sporadic episodes of pluri-annual variability.

3.4. SSWEI: Relationships with teleconnection patterns

The Pearson correlation coefficients computed between the monthly teleconnection indices (NAO, WNAO, AO, and AMO) and *SSWEI*, over the entire period 1930–2020, are shown in Figure S2. Correlations in Figure S2 are performed on 7-year moving-averaged data to highlight pluriannual response of *SSWEI* to climatic and teleconnection forcings. NAO, WNAO, and AO showed significant, negative correlations (anti-correlation) with *SSWEI* during the early snow season, particularly in January, considering all elevation bands. Differently, AMO significantly anticorrelated with *SSWEI* during the late snow season, especially in March, considering the three elevation bands. These results highlight that higher (lower) NAO, WNAO, AO, and AMO values are linked to lower (higher) *SSWEI* values.

From the correlation analysis, we selected the months with the highest correlation coefficients to be used in the WTC analysis. We selected January for NAO, WNAO, and AO, and March for the AMO. Given the similar behaviour of NAO and WNAO, and considering the higher correlation coefficients for WNAO, we applied the WTC only on WNAO. The results of the WTC analysis are reported in Fig. 6. The low and medium elevation bands had a similar behaviour. For both WNAO and AO, looking at the pluri-decadal variability, the coherence with *SSWEI* was strong (close to 1) until the 1980s, then the signal became weaker and not significant (except for AO, at the medium elevations). This break was followed by a coherence increase after 2000, displaying also a shift towards a decadal variability. AO also showed some significant signals below the decadal time scale, which vanished around the 1980s. At the medium elevations, looking at the pluri-decadal variability, the coherence between AMO and *SSWEI* was strong until the end of the 1980s, then it vanished (we found no persistent, significant signal for AMO at low elevation). Differently from the low and medium elevation bands, at the high elevations all teleconnection indices showed persistently strong coherence at the pluri-decadal time scale. However, during the 1980s, AO showed a shift from a pluri-decadal to decadal variability and the vanishing of some significant, pluri-annual signals.

The Pearson correlation coefficients computed between the monthly teleconnection indices and *AT** and *SPI* are shown in Figure S2. For this analysis, we discriminated between two sub-periods, 1950–1990 and 1991–2020, due to the step-like change that occurred in *AT** at the end of the 1980s - beginning of the 1990s (Fig. 4). In January, NAO, WNAO, and AO were significantly and positively correlated with *AT** in the period 1950–1990, while the correlation weakened in the sub-period 1991–2020 (the correlation vanished for AO). Differently, we did not find significant correlations between NAO, WNAO, and AO and *SPI* for January, except for a significant, negative correlation for AO in the period 1991–2020. In March, *AT** did not significantly correlate with AMO both in 1950–1990 and 1991–2020, while *SPI* showed a significant, negative correlation in the period 1950–1990.

4. Discussion

4.1. Variability of SSWEI

Our results show a marked variability in monthly *SSWEI* through the analysed period (1930–2020). Previous studies on *SWE* variability and trend in the European Alps reported: (i) a general reduction in February (weaker) and April (stronger) *SWE* across the Alpine chain in the period 1968–2012 (Marty et al., 2017) as well as a spring *SWE* decrease occurring between 1965 and 2007 in the Italian Alps (Bocchiola and Diolaiuti, 2010), (ii) weak nonsignificant *SWE* decreases in the period 1981–2010, across the entire Alpine chain (Mudryk et al., 2015); (iii) no *SWE* trends in the Swiss Alps for the period 1975–1992 (Rohrer et al., 1994). The apparent disagreement among the previously presented research results (including our findings) are likely caused by the different periods and datasets considered by the authors. For instance, Marty et al. (2017) investigated a long-term (1945–2012), Alpine-wide *SWE* time series by calculating the relative February and April *SWE* deviation from its long-term mean (1961–90), for different stations across the Alps. Their findings show several agreements with ours, such

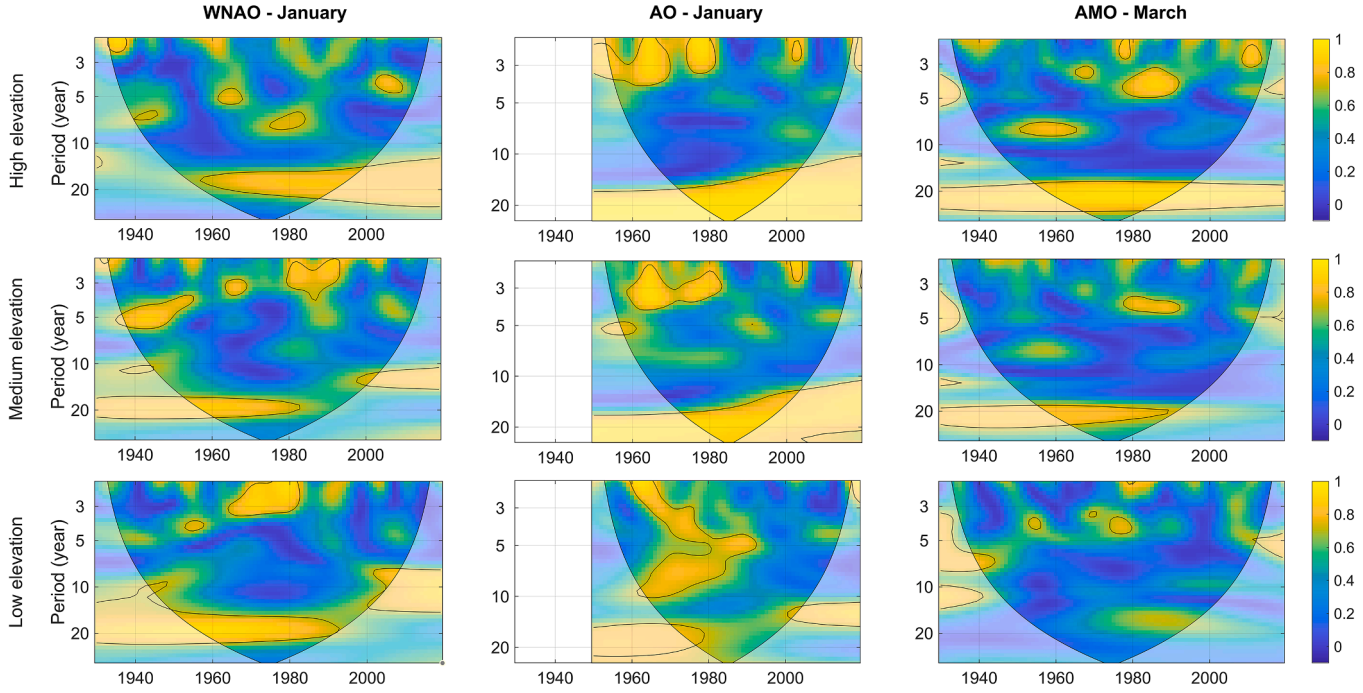

Fig. 6. WTC of selected monthly teleconnection indices with *SSWEI*. The 95% level of confidence is reported in full black line.

as: (i) in February, lowermost values in the early 1990s and partial recovery/stabilisation in the following decades, highermost values in the 1970s-1980s, and some kind of stationarity with relatively low-magnitude oscillations in the previous decades; (ii) in April, lowermost values in the early 1990s with a following partial stabilisation, highermost values in the 1970s-1980s, and low values in the 1940s-1950s.

The most striking changes occurred in the period 1991–2020, that generally experienced record-low *SSWEI* values across all elevation bands (although we also found few low monthly *SSWEI* values in the 1940s-1950s). It is worth noting, though, that these changes did no occurred gradually, but rather following a sharp drop culminating in the early 1990s (especially in spring). The abrupt change in *SWE* values between the end of the 1980s and the early 1990s was also measured in the observational *SWE* data collected by Marty et al. (2017), across the European Alps. This evidence is also in agreement with the findings that other studies have reported, showing a step-like change for Alpine *HS* occurring in the late 1980s - early 1990s (Marty, 2008; Durand et al., 2009; Valt and Cianfarra, 2010; Matiu et al., 2021). Our results showed that this drop was then followed by a partial stabilisation or even recovery, although *SSWEI* values remained mostly negative until the end of the investigated period. This is also in agreement with previous studies on snow cover in the Alps, reporting that the monthly mean snow-covered area across the Alpine chain has not decreased significantly since the step change (Hüsler et al., 2014). However, in an Alpine-wide view, this temporal variability is also accompanied by a strong regional variability, when considering *HS* (Matiu et al., 2021).

Snow drought has been firstly defined as near- or above average accumulated precipitation coinciding with below-average *SWE* at a point in time (Pederson et al. 2011). Some studies have distinguished between dry (i.e., precipitation limited) and (i.e., temperature driven, despite above-normal precipitation) snow droughts (Harpold et al., 2017; Hatchett and McEvoy, 2018). In our work, we consider all types of snow droughts without differentiating them. In our study region, unprecedented and persistent snow-drought conditions occurred in the period 1991–2020 (Fig. 7). Particularly low *SWE* values in the last two to three decades have been reported not only for the Alps (Marty et al., 2017), but also for other low- to high-mountainous areas of the world such as: Europe (Dong and Menzel, 2020; Nedelcev and Jenicek, 2021), North America (Mote et al., 2018), and Asia (Kraaijenbrink et al., 2021). Finally, in the last few decades, several areas of the world emerged as hot spots for snow droughts (including Europe), showing longer snow drought durations, although high continental and regional variability exists (Huning and AghaKouchak, 2020). Thus, our evidence seems to be part of a world-wide pattern, rather than of a region-specific one, indicating recent, persistent *SWE* deficits.

4.2. Drivers of SSWEI variability

SSWEI variability seemed to be generally interconnected to precipitation variability, here analysed through the *SPI*. However, this interconnection weakened in the period 1991–2020, especially at medium (March-April) and high elevation (November-April-May), although also the low elevation band showed a divergent behaviour in the 2010s (January–March). Indeed, negative *SSWEI* trends got decoupled from - slightly negative to positive - *SPI* trends, under the effect of strongly positive *AT** trends. The observed changes were likely caused by more frequent and more intense melt (Klein et al., 2016), and by a shift from solid to liquid precipitation (Serquet et al., 2011; Nikolova et al., 2013), both resulting from higher air temperatures during winter and spring (Beniston et al., 2018). In addition, during the early 1990s, we found concomitant strong air temperature increases and - slight to moderate - precipitation decreases, resulting in unprecedented negative *SSWEI* trends. This regime shift, mostly involving air temperature, has been documented both at the Alpine (Marty, 2008) and global (Reid et al., 2016) scales. In addition, our results clearly showed the importance of *AT** variations in decoupling *SSWEI* from *SPI* in other periods, such as in the 1960s (January, all elevation bands) and 1970s-1980s (April, medium and high elevation), when positive *SSWEI* was associated to negative *SPI* and *AT**.

Regarding the correlation between *SSWEI* and the investigated teleconnection indices, we found high (and significant) negative coefficients across the entire period 1930–2020. Considering the three elevation bands, we found the strongest anticorrelations for NAO, WNAO, and AO to occur in January (during the early snow season, i.e., accumulation phase), while for AMO the strongest anticorrelation occurred in March (late snow season, i.e., melting phase). These results are in agreement with a large body of literature. Indeed, in the southern European Alps, in Italy, a common pattern seemed to emerge, with snow and winter precipitation dynamics being negatively correlated with NAO/WNAO (Maragno et al., 2009; Bocchiola and Diolaiuti, 2010; Diolaiuti et al., 2012; Terzago et al., 2013; Brugnara and Maugeri, 2019), AMO (Zampieri et al., 2013; Brugnara and Maugeri, 2019), and AO (Terzago et al., 2013); similar results were found for NAO and winter mass balance of glaciers (Carturan et al., 2015). In addition, other studies in the European Alps have found NAO to be negatively (positively) correlated with winter precipitation (Quadrelli et al., 2001; López-Moreno et al., 2011) (temperature) (Beniston, 1997; Beniston and Jungo, 2002), snow cover (Henderson and Leathers, 2010), and mass balance of glaciers (Reichert et al., 2001). AMO has also been reported to be anticorrelated with glacier mass balance (Huss et al., 2010). However, the WTC analysis showed changes/breaks in coherence and shifts in time-scale variability occurring mostly throughout the 1980s, sometimes with the total vanishing of the coherence afterwards, especially at

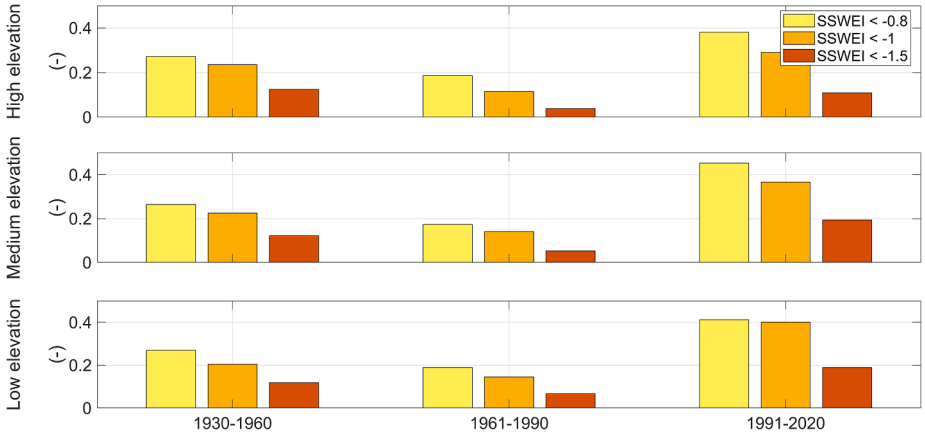

Fig. 7. Mean frequency of monthly events below selected *SSWEI* thresholds, during the snow season, by elevation groups.

low and medium elevations. In the same period, *AT** skyrocketed (*SPI* remained more stable), reaching the highest values and showing the most significant trends. This occurrence further highlights the sensitivity of low and medium elevations towards climate changes (Marcolini et al., 2017b), where it is likely that the atmospheric warming occurring in the last decades has played an increasingly important role in driving *SWE* (Marty et al., 2017) and snow dynamics (Hock et al., 2019).

4.3. Hydrological implications and research perspectives

The decrease of water storage in the snowpack can potentially have dire implications for water supply in those communities that directly rely on snow melting (IPCC, 2019), with relevant regional and global ramifications also in downstream snow-free areas (Huning and AghaKouchak, 2020). The magnitude of these implications will likely increase in the future. For instance, for the European Alps, at an elevation of 1500 m a.s.l., it has been simulated a reduction in *SWE* of up to 80–90 % by the end of the century, while the decrease has been projected to be more reduced (10 %) for elevations above 3000 m a.s.l. (Rousselot et al., 2012; Steger et al., 2013; Schmucki et al., 2015). Thus, human activities are being and will be even more influenced by the ongoing and anticipated changes, with relevant impacts on water management (Laghari et al., 2012; Köplin et al., 2014) regarding, for instance, water supply, hydropower production and irrigation requirements (Barnett et al., 2005; Gaudard and Romerio, 2014; Gaudard et al., 2014; Hill Clarvis et al., 2014; Qin et al., 2020).

The 2021–2022 drought event that impacted (and that is still impacting at the beginning of September 2022) the Po River basin is a clear example of the implications of our findings. Preliminary data collected by the Autorità di Bacino Distrettuale del Fiume Po (District Basin Authority of the Po River) showed that Winter 2021–2022 was characterised by a significant precipitation deficit (*SPI*3 constantly below –1.5) over several areas of the Western and Central Italian Alps. The lack of solid precipitation during winter, along with a persistent precipitation deficit during spring and summer (*SPI*3 $<$ –1.5) and air temperatures above the seasonal means, resulted in an unprecedented hydrological drought. The Po River discharge, at the Pontelagoscuro monitoring station, was –60 % (with respect of the long-term monthly average) in March and –85 % in July. Due to the very low discharge of several rivers, not sustained by the spring snow melt, the agricultural sector was particularly affected. The drought event that impacted the Po River basin in 2022 clearly shows that a better understanding of the snowpack dynamics can strongly support the management of the entire Po basin, both over short periods and over medium to long periods.

It is also worth noting the importance of estimating the historical *SWE* time series in terms of standardised indices: significant changes of the *SSWEI* point out significant changes in the "average hydrological conditions", indicating the range of a "new normality" that must be taken into account for implementing sound and effective mitigation measures and strategy plans. In this framework, the study of the emerging phenomenon known as snow drought will be more and more relevant (Cooper et al., 2016; Mote et al., 2016; Huning and AghaKouchak, 2020; Hatchett et al., 2022). Even more important will be the understanding of the hydrometeorological processes that could cause snow droughts, in order to evaluate their impacts on consumptive uses that rely on snowmelt-derived runoff or ecological processes that depend on the presence of a snowpack (Hatchett and McEvoy, 2018). In that perspective, decision support could benefit from further investigations on the current response to teleconnection indices based on wider station networks.

5. Conclusions

We assessed the long-term (1930–2020) variability of monthly *SSWEI* across the Italian Alps and its links with climate change and large-scale atmospheric forcings, using modelled *SWE* derived from daily *HS* data. We found record-low monthly *SSWEI* values to occur mainly in the last few decades (1991–2020), irrespective of elevation, although some other negative *SSWEI* oscillations occurred during the investigated period. Lowermost values were experienced in the early 1990s and, despite a partial recovery or stabilisation in the following years/decades, *SSWEI* remained generally negative until 2020, especially at the snow season tails. We investigated the role of large-scale atmospheric forcings (teleconnection indices) in driving these patterns, finding that NAO, WNAO, AMO, and AO were anticorrelated with *SSWEI*, during different phases of the snow season. However, strong changes/breaks occurred in the relations between teleconnection indices and *SSWEI* after the 1980s, especially at low and medium elevations. We also looked at the relationships between climate drivers, precipitation (*SPI*) and air temperature (*AT**), and *SSWEI*, finding that *SSWEI* variability seemed to be generally interconnected to precipitation variability. However, this interconnection was lost mostly in the period 1991–2020, when highly positive *AT** occurred. Therefore, increasing air temperature has likely become predominant over the influence of large-scale atmospheric forcings and precipitation variability in the recent decades. We conclude that snow drought variability is an important indicator of climate change, and that the unprecedented and persistent snow-drought conditions in the last decades could have deep influence on water management in the southern Alpine area.

Declaration of Competing Interest

The authors declare that they have no known competing financial interests or personal relationships that could have appeared to influence the work reported in this paper.

Data availability

Data will be made available on request.

Acknowledgments

We wish to thank Anna Bruna Petrangeli for her help in data elaboration. This research was partially funded by the INTERREG V-B Adriatic-Ionian ADRION Programme 2014–2020 - Second Call for Proposal - Priority Axis 2 (project MUHA - Multihazard Framework for Water related risks management, n. 952). *HS* data have been provided in the framework of the agreement between IRSA-CNR and ARPA Veneto of 09/11/2018 (prot. IRSA 2018/0004867). We are grateful to the Editor, Associate Editor, and two reviewers who provided valuable feedback and input during the review of this manuscript.

Appendix A. Supplementary data

Supplementary data to this article can be found online at https://doi.org/10.1016/j.jhydrol.2022.128532.

References

Auer, I., Böhm, R., Jurkovic, A., et al., 2007. HISTALP-historical instrumental climatological surface time series of the Greater Alpine Region. Int. J. Climatol. 27, 17–46. https://doi.org/10.1002/joc.1377.

Avanzi, F., De Michele, C., Ghezzi, A., 2015. On the performances of empirical regressions for the estimation of bulk snow density. Geogr. Fis. Din. Quat. 38, 105–112. https://doi.org/10.4461/GFDQ.2015.38.10.

Barfod, E., Müller, K., Saloranta, T., et al., 2013. The expert tool XGEO and its applications in the Norwegian Avalanche Forecasting Service. In: International Snow Science Workshop Grenoble, Chamonix Mont-Blanc, 7–11. https://arc.lib.montana.edu/snow-science/objects/ISSW13_paper_P1-13.pdf.

Barnett, T.P., Adam, J.C., Lettenmaier, D.P., 2005. Potential impacts of a warming climate on water availability in snow-dominated regions. Nature 438, 303–309. https://doi.org/10.1038/nature04141.

Bartolini, E., Claps, P., D'Odorico, P., 2009. Interannual variability of winter precipitation in the European Alps: relations with the North Atlantic Oscillation. Hydrol. Earth Syst. Sci. 13, 17–25. https://doi.org/10.5194/hess-13-17-2009.

Bartolini, E., Claps, P., D'Odorico, P., 2010. Connecting European snow cover variability with large scale atmospheric patterns. Adv. Geosci. 26, 93–97. https://doi.org/10.5194/adgeo-26-93-2010.
Beniston, M., 1997. Variations of Snow Depth and Duration in the Swiss Alps Over the Last 50 Years: Links to Changes in Large-Scale Climatic Forcings. In: Diaz, H.F., Beniston, M., Bradley, R.S. (Eds.), Climatic Change at High Elevation Sites. Springer, Dordrecht. https://doi.org/10.1007/978-94-015-8905-5_3.
Beniston, M., 2012. Impacts of climatic change on water and associated economic activities in the Swiss Alps. J. Hydrol. 412–413, 291–296. https://doi.org/10.1016/j.jhydrol.2010.06.046.
Beniston, M., Jungo, P., 2002. Shifts in the distributions of pressure, temperature and moisture and changes in the typical weather patterns in the Alpine region in response to the behavior of the North Atlantic Oscillation. Theor. Appl. Climatol. 71, 29–42. https://doi.org/10.1007/s704-002-8206-7.
Beniston, M., Farinotti, D., Stoffel, M., et al., 2018. The European mountain cryosphere: a review of its current state, trends, and future challenges. Cryosphere 12, 759–794. https://doi.org/10.5194/tc-12-759-2018.
Berni, A., Giancanelli, E., 1966. La campagna dirilievi nivometrici effettuata dall'ENEL nel periodo febbraio – giugno 1966. Energia Elettrica 9, 533–542.
Blasi, C., Capotorti, G., Copiz, R., et al., 2014. Classification and mapping of the ecoregions of Italy. Plant Biosyst. 148 (6), 1255–1345. https://doi.org/10.1080/11263504.2014.985756.
Bocchiola, D., Diolaiuti, G., 2010. Evidence of climate change within the Adamello Glacier of Italy. Theor. Appl. Climatol. 100, 351–369. https://doi.org/10.1007/s00704-009-0186-x.
Brugnara, Y., Maugeri, M., 2019. Daily precipitation variability in the southern Alps since the late 19th century. Int. J. Climatol. 39 (8), 3492–3504. https://doi.org/10.1002/joc.6034.
Carturan, L., Baroni, C., Brunetti, M., et al., 2015. Analysis of the mass balance time series of glaciers in the Italian Alps. Cryosphere 10, 695–712- https://doi.org/10.5194/tc-10-695-2016.
Cooper, M.G., Nolin, A.W., Safeeq, M., 2016. Testing the recent snow drought as an analog for climate warming sensitivity of Cascades snowpacks. Environ. Res. Lett. 11, 084009 https://doi.org/10.1088/1748-9326/11/8/084009.
De Michele, C., Avanzi, F., Ghezzi, A., et al., 2013. Investigating the dynamics of bulk snow density in dry and wet conditions using a one-dimensional model. Cryosphere 7, 433–444. https://doi.org/10.5194/tc-7-433-2013.
Dee, D.P., Uppala, S.M., Simmons, A.J., et al., 2011. The ERA-Interim reanalysis: configuration and performance of the data assimilation system. Q. J. R. Meteorol. Soc. 137 (656), 553–597. https://doi.org/10.1002/qj.828.
Diolaiuti, G., Bocchiola, D., D'agata, C., et al., 2012. Evidence of climate change impact upon glaciers' recession within the Italian Alps. Theor. Appl. Climatol. 109, 429–445. https://doi.org/10.1007/s00704-012-0589-y.
Dong, C., Menzel, L., 2020. Recent snow cover changes over central European low mountain ranges. Hydrol. Process. 34 (2), 321–338. https://doi.org/10.1002/hyp.13586.
Dozier, J., Bair, E., Davis, R., 2016. Estimating the spatial distribution of snow water equivalent in the world's mountains. Wiley Interdiscip. Rev. Water 3 (3), 461–474. https://doi.org/10.1002/wat2.1140.
Durand, Y., Giraud, G., Laternser, M., et al., 2009. Reanalysis of 47 Years of Climate in the French Alps (1958–2005): Climatology and Trends for Snow Cover. J. Appl. Meteorol. Climatol. 48 (12), 2487–2512. https://doi.org/10.1175/2009JAMC1810.1.
Egli, L., Jonas, T., Meister, R., 2009. Comparison of different automatic methods for estimating snow water equivalent. Cold Reg. Sci. Technol. 57 (2–3), 107–115. https://doi.org/10.1016/j.coldregions.2009.02.008.
Elias, E., James, D., Heimel, S., et al., 2021. Implications of observed changes in high mountain snow water storage, snowmelt timing and melt window. J. Hydrol. Reg. Stud. 35, 100799 https://doi.org/10.1016/j.ejrh.2021.100799.
Essery, R., Morin, S., Lejeune, Y., et al., 2013. A comparison of 1701 snow models using observations from an alpine site. Adv. Water Resour. 55, 131–148. https://doi.org/10.1016/j.advwatres.2012.07.013.
Fierz, C.R., Armstrong, R.L., Durand, Y., et al., 2009. The international classification for seasonal snow on the ground. International Hydrological Programme of the United Nations Educational, Scientific and Cultural Organization (UNESCO-IHP), Paris, IHP Technical Documents in Hydrology No. 83, IACS Contribution No. 1. https://cryosphericsciences.org/publications/snow-classification/.
Freppaz, M., Pintaldi, E., Magnani, A., et al., 2018. Topsoil and snow: a continuum system. Appl. Soil Ecol. 123, 435–440. https://doi.org/10.1016/j.apsoil.2017.06.029.
Gaudard, L., Romerio, F., 2014. The future of hydropower in Europe: interconnecting climate, markets and policies. Environ. Sci. Policy 37, 172–181. https://doi.org/10.1016/j.envsci.2013.09.008.
Gaudard, L., Romerio, F., Dalla Valle, F., et al., 2014. Climate change impacts on hydropower in the Swiss and Italian Alps. Sci. Total Environ. 493, 1211–1221. https://doi.org/10.1016/j.scitotenv.2013.10.012.
Gerstengarbe, F.W., Werner, P.C., 1999. Estimation of the beginning and end of recurrent events within a climate regime. Clim. Res. 11, 97–107. https://doi.org/10.3354/cr011097.
Grossmann, A., Morlet, J., 1984. Decomposition of Hardy functions into square integrable wavelets of constant shape. SIAM J. Math. Anal. 15, 723–736. https://doi.org/10.1137/0515056.
Guyennon, N., Romano, E., Portoghese, I., et al., 2013. Benefits from using combined dynamical-statistical downscaling approaches – lessons from a case study in the Mediterranean region. Hydrol. Earth Syst. Sc. 17, 705–720. https://doi.org/10.5194/hess-17-705-2013.
Guyennon, N., Valerio, G., Salerno, F., et al., 2014. Internal wave weather heterogeneity in a deep multi-basin subalpine lake resulting from wavelet transform and numerical analysis. Adv. Water Resour. 71, 149–161. https://doi.org/10.1016/j.advwatres.2014.06.013.
Guyennon, N., Valt, M., Salerno, F., et al., 2019. Estimating the snow water equivalent from snow depth measurements in the Italian Alps. Cold Reg. Sci. Technol. 167, 102859 https://doi.org/10.1016/j.coldregions.2019.102859.
Harpold, A.A., Dettinger, M., Rajagopal, S., 2017. Defining snow drought and why it matters. Eos, Trans. Amer. Geophys. Union 98. https://doi.org/10.1029/2017EO068775.
Hatchett, B.J., Burak, S., Rutz, J.J., et al., 2017. Avalanche fatalities during atmospheric river events in the western United States. J. Hydrometeorol. 18 (5), 1359–1374. https://doi.org/10.1175/JHM-D-16-0219.1.
Hatchett, B.J., McEvoy, D.J., 2018. Exploring the origins of snow drought in the northern Sierra Nevada. California. Earth Interact. 22, 1–13. https://doi.org/10.1175/EI-D-17-0027.1.
Hatchett, B.J., Rhoades, A.M., McEvoy, D.J., 2022. Monitoring the daily evolution and extent of snow drought. Nat. Hazards Earth Syst. Sci. 22, 869–890. https://doi.org/10.5194/nhess-22-869-2022.
Henderson, G.R., Leathers, D.J., 2010. European snow cover extent variability and associations with atmospheric forcings. Int. J. Climatol. 30, 1440–1451. https://doi.org/10.1002/joc.1990.
Hill, D.F., Burakowski, E.A., Crumley, R.L., et al., 2019. Converting snow depth to snow water equivalent using climatological variables. Cryosphere 13, 1767–1784. https://doi.org/10.5194/tc-13-1767-2019.
Hill Clarvis, M., Fatichi, S., Allan, A.A., et al., 2014. Governing and managing water resources under changing hydro-climatic contexts: The case of the Upper Rhone Basin. Environ. Sci. Pol. 43, 56–67. https://doi.org/10.1016/j.envsci.2013.11.005.
Hock, R., Rasul, G., Adler, C., et al., 2019. High Mountain Areas. In: IPCC Special Report on the Ocean and Cryosphere in a Changing Climate [Pörtner, H.-O., Roberts, D.C., Masson-Delmotte, V., et al., (eds.)], Cambridge University Press, Cambridge, UK and New York, NY, USA, 131–202. https://doi.org/10.1017/9781009157964.004.
Huning, L.S., AghaKouchak, A., 2020. Global snow drought hot spots and characteristics. Proc. Natl. Acad. Sci. U.S.A. 117 (33), 19753–19759. https://doi.org/10.1073/pnas.1915921117.
Hurrell, J.W., 1995. Decadal trends in the North Atlantic Oscillation: regional temperatures and precipitation. Science 269 (5224), 676–679. https://doi.org/10.1126/science.269.5224.676.
Hüsler, F., Jonas, T., Riffler, M., et al., 2014. A satellite-based snow cover climatology (1985–2011) for the European Alps derived from AVHRR data. Cryosphere 8, 73–90. https://doi.org/10.5194/tc-8-73-2014.
Huss, M., Hock, R., Bauder, A., et al., 2010. 100-year mass changes in the Swiss Alps linked to the Atlantic Multidecadal Oscillation. Geophys. Res. Lett. 37, L10501. https://doi.org/10.1029/2010GL042616.
Huss, M., Bookhagen, B., Huggel, C., et al., 2017. Toward mountains without permanent snow and ice. Earth's Future 5 (5), 418–435. https://doi.org/10.1002/2016EF000514.
Immerzeel, W.W., van Beek, L.P.H., Bierkens, M.F.P., 2010. Climate change will affect the Asian water towers. Science 328, 1382–1385. https://doi.org/10.1126/science.1183188.
IPCC, 2019. IPCC Special Report on the Ocean and Cryosphere in a Changing Climate [Pörtner, H.-O., Roberts, D.D., Masson-Delmotte, V., et al. (eds.)], Cambridge University Press, Cambridge, UK and New York, NY, USA. https://doi.org/10.1017/9781009157964.
Isotta, F.A., Frei, C., Weilguni, V., et al., 2014. The climate of daily precipitation in the Alps: development and analysis of a high-resolution grid dataset from pan-Alpine rain-gauge data. Int. J. Climatol. 34 (5), 1657–1675. https://doi.org/10.1002/joc.3794.
Jonas, T., Rixen, C., Sturm, M., et al., 2008. How alpine plant growth is linked to snow cover and climate variability. J. Geophys. Res. 113, G03013. https://doi.org/10.1029/2007JG000680.
Jonas, T., Marty, C., Magnusson, J., 2009. Estimating the snow water equivalent from snow depth measurements in the Swiss Alps. J. Hydrol. 378 (1–2), 161–167. https://doi.org/10.1016/j.jhydrol.2009.09.021.
Jörg-Hess, S., Griessinger, N., Zappa, M., 2015. Probabilistic Forecasts of Snow Water Equivalent and Runoff in Mountainous Areas. J. Hydrometeorol. 16 (5), 2169–2186. https://doi.org/10.1175/JHM-D-14-0193.1.
Kaplan, A., Cane, M., Kushnir, Y., et al., 1998. Analyses of global sea surface temperature 1856–1991. J. Geophys. Res. 103 (C9), 18567–18589. https://doi.org/10.1029/97JC01736.
Keller, F., Goyette, S., Beniston, M., 2005. Sensitivity Analysis of Snow Cover to Climate Change Scenarios and Their Impact on Plant Habitats in Alpine Terrain. Climatic Change 72, 299–319. https://doi.org/10.1007/s10584-005-5360-2.
Kendall, M.G., 1975. Rank Correlation Methods. Oxford University Press, New York.
Kinar, N.J., Pomeroy, J.W., 2015. Measurement of the physical properties of the snowpack. Rev. Geophys. 53 (2), 481–544. https://doi.org/10.1002/2015RG000481.
Klein, G., Vitasse, Y., Rixen, C., et al., 2016. Shorter snow cover duration since 1970 in the Swiss Alps due to earlier snowmelt more than later snow onset. Climatic Change 139, 637–649. https://doi.org/10.1007/s10584- 016-1806-y.
Köplin, N., Rößler, O., Schädler, B., et al., 2014. Robust estimates of climate-induced hydrological change in a temperate mountainous region. Climatic Change 122, 171–184. https://doi.org/10.1007/s10584-013-1015-x.
Kraaijenbrink, P.D.A., Stigter, E.E., Yao, T., et al., 2021. Climate change decisive for Asia's snow meltwater supply. Nat. Clim. Chang. 11, 591–597. https://doi.org/10.1038/s41558-021-01074-x.

Laghari, A.N., Vanham, D., Rauch, W., 2012. To what extent does climate change result in a shift in Alpine hydrology? A case study in the Austrian Alps. Hydrolog. Sci. J. 57, 103–117. https://doi.org/10.1080/02626667.2011.637040.
Larue, F., Royer, A., De Sève, D., et al., 2017. Validation of GlobSnow-2 snow water equivalent over Eastern Canada. Remote Sens. Environ. 194, 264–277. https://doi.org/10.1016/j.rse.2017.03.027.
Li, J., Wang, J., 2003. A modified zonal index and its physical sense. Geophys. Res. Lett. 30 (12), 1632–1636. https://doi.org/10.1029/2003GL017441.
Li, D., Wrzesien, M.L., Durand, M., et al., 2017. How much runoff originates as snow in the western United States, and how will that change in the future? Geophys. Res. Lett. 44, 6163–6172. https://doi.org/10.1002/2017GL073551.
López-Moreno, J.I., Vicente-Serrano, S.M., Morán-Tejeda, E., et al., 2011. Effects of the North Atlantic Oscillation (NAO) on combined temperature and precipitation winter modes in the Mediterranean mountains: Observed relationships and projections for the 21st century. Glob. Planet. Change 77 (1–2), 62–76. https://doi.org/10.1016/j.gloplacha.2011.03.003.
López-Moreno, J.I., Leppänen, L., Luks, B., et al., 2020. Intercomparison of measurements of bulk snow density and water equivalent of snow cover with snow core samplers: Instrumental bias and variability induced by observers. Hydrol. Process. 34, 3120–3133. https://doi.org/10.1002/hyp.13785.
Lucianetti, G., Cianfarra, P., Mazza, R., 2017. Lineament domain analysis to infer groundwater flow paths: Clues from the Pale di San Martino fractured aquifer, Eastern Italian Alps. Geosphere 13 (5), 1729–1746. https://doi.org/10.1130/GES01500.1.
Magnusson, J., Nævdal, G., Matt, F., et al., 2020. Improving hydropower inflow forecasts by assimilating snow data. Hydrol. Res. 51 (2), 226–237. https://doi.org/10.2166/nh.2020.025.
Maragno, D., Diolaiuti, G., D'agata, C., et al., 2009. New evidence from Italy (Adamello Group, Lombardy) for analysing the ongoing decline of Alpine glaciers. Geogr. Fis. Din. Quat. 32, 31–39. http://gfdq.glaciologia.it/032_1_04_2009/.
Marazzi, S., 2005. Atlante orografico delle Alpi. SOIUSA. suddivisione orografica internazionale unificata del sistema alpino. Priuli & Verlucca.
Marcolini, G., Bellin, A., Chiogna, G., 2017a. Performance of the Standard Normal Homogeneity Test for the homogenization of mean seasonal snow depth time series. Int. J. Climatol. 37, 1267–1277. https://doi.org/10.1002/joc.4977.
Marcolini, G., Bellin, A., Disse, M., et al., 2017b. Variability in snow depth time series in the Adige catchment. J. Hydrol. Reg. Stud. 13, 240–254. https://doi.org/10.1016/j.ejrh.2017.08.007.
Marcolini, G., Koch, R., Chimani, B., et al., 2019. Evaluation of homogenization methods for seasonal snow depth data in the Austrian Alps, 1930–2010. Int. J. Climatol. 39, 4514–4530. https://doi.org/10.1002/joc.6095.
Margulis, S.A., Cortés, G., Girotto, M., et al., 2016. Characterizing the extreme 2015 snowpack deficit in the Sierra Nevada (USA) and the implications for drought recovery. Geophys. Res. Lett. 43, 6341–6349. https://doi.org/10.1002/2016GL068520.
Marty, C., 2008. Regime shift of snow days in Switzerland. Geophys. Res. Lett. 35, L12501. https://doi.org/10.1029/2008GL033998.
Marty, C., Tilg, A.-M., Jonas, T., 2017. Recent evidence of large scale receding snow water equivalents in the European Alps. J. Hydrometeorol. 18, 1021–1031. https://doi.org/10.1175/JHM-D-16-0188.1.
Matiu, M., Crespi, A., Bertoldi, G., et al., 2021. Observed snow depth trends in the European Alps: 1971 to 2019. Cryosphere 15, 1343–1382. https://doi.org/10.5194/tc-15-1343-2021.
McKee, T.B., Doesken, N.J., Kleist, K., 1993. The relationship of drought frequency and duration to time scale. In: Proceedings of the 8th Conference on Applied Climatology, Anaheim, CA, USA, 17–22 January 1993. Boston, MA: American Meteor. Society.
Mote, P.W., Rupp, D.E., Li, S., et al., 2016. Perspectives on the causes of exceptionally low 2015 snowpack in the western United States. Geophys. Res. Lett. 43, 10980–10988. https://doi.org/10.1002/2016GL069965.
Mote, P.W., Li, S., Lettenmaier, D.P., et al., 2018. Dramatic declines in snowpack in the western US. Npj Clim. Atmos. Sci. 1 (1), 2. https://doi.org/10.1038/s41612-018-0012-1.
Mudryk, L.R., Derksen, C., Kushner, P.J., et al., 2015. Characterization of Northern Hemisphere snow water equivalent datasets, 1981–2010. J. Climate 28, 8037–8051. https://doi.org/10.1175/JCLI-D-15-0229.1.
Muñoz-Sabater, J., Dutra, E., Agustí-Panareda, A., et al., 2021. ERA5-Land: A state-of-the-art global reanalysis dataset for land applications. Earth Syst. Sci. Data 13, 4349–4383. https://doi.org/10.5194/essd-13-4349-2021.
Nedelcev, O., Jenicek, M., 2021. Trends in seasonal snowpack and their relation to climate variables in mountain catchments in Czechia. Hydrol. Sci. J. 66 (16), 2340–2356. https://doi.org/10.1080/02626667.2021.1990298.
Nicolet, G., Eckert, N., Morin, S., et al., 2016. Decreasing spatial dependence in extreme snowfall in the French Alps since 1958 under climate change. J. Geophys. Res.-Atmos. 121, 8297–8310. https://doi.org/10.1002/2016JD025427.
Nicolet, G., Eckert, N., Morin, S., et al., 2018. Assessing Climate Change Impact on the Spatial Dependence of Extreme Snow Depth Maxima in the French Alps. Water Resour. Res. 54 (10), 7820–7840. https://doi.org/10.1029/2018WR022763.
Nikolova, N., Faško, P., Lapin, M., et al., 2013. Changes in snowfall/precipitation-day ratio in Slovakia and their linkages with air temperature and precipitation. Contrib. Geophys. Geod. 43, 141–155. https://doi.org/10.2478/congeo-2013-0009.
Pauli, H., Gottfried, M., Hohenwallner, D., et al., 2005. Ecological climate impact research in high mountain environments: GLORIA (Global Observation Research Initiative in Alpine Environments) - its roots, purpose and long-term perspectives. In: Global Change and Mountain Regions, Springer, Dordrecht, 383–391. https://link.springer.com/chapter/10.1007%2F1-4020-3508-X_38.
Pederson, G.T., Gray, S.T., Woodhouse, C.A., et al., 2011. The unusual nature of recent snowpack declines in the North American cordillera. Science 333, 332–335. https://doi.org/10.1126/science.1201570.
Pistocchi, A., 2016. Simple estimation of snow density in an Alpine region. J. Hydrol.: Reg. Stud. 6, 82–89. https://doi.org/10.1016/j.ejrh.2016.03.004.
Qin, Y., Abatzoglou, J.T., Siebert, S., et al., 2020. Agricultural risks from changing snowmelt. Nat. Clim. Chang. 10, 459–465. https://doi.org/10.1038/s41558-020-0746-8.
Quadrelli, R., Lazzeri, M., Cacciamani, C., et al., 2001. Observed winter Alpine precipitation variability and links with large-scale circulation patterns. Clim. Res. 17, 275–284. https://doi.org/10.3354/cr017275.
Reichert, B.K., Bengtsson, L., Oerlemans, J., 2001. Midlatitude Forcing Mechanisms for Glacier Mass Balance Investigated Using General Circulation Models. J. Clim. 3767–3784 https://doi.org/10.1175/1520-0442(2001)014<3767:MFMFGM>2.0.CO;2.
Reid, P.C., Hari, R.E., Beaugrand, G., et al., 2016. Global impacts of the 1980s regime shift. Global Change Biol. 22, 682–703. https://doi.org/10.1111/gcb.13106.
Rixen, C., Teich, M., Lardelli, C., et al., 2011. Winter Tourism and Climate Change in the Alps: An Assessment of Resource Consumption, Snow Reliability, and Future Snowmaking Potential. Mt. Res. Dev. 31 (3), 229–236. https://doi.org/10.1659/MRD-JOURNAL-D-10-00112.1.
Rohrer, M.B., Braun, L.N., Lang, H., 1994. Long-term records of the snow cover water equivalent in the Swiss Alps: 1. Analysis. Nord. Hydrol. 25 (1–2), 53–64. https://doi.org/10.2166/nh.1994.0019.
Romano, E., Petrangeli, A.B., Salerno, F., et al., 2021. Do recent meteorological drought events in central Italy result from long-term trend or increasing variability? Int. J. Climatol. 42 (7), 4111–4128. https://doi.org/10.1002/joc.7487.
Rousselot, M., Durand, Y., Giraud, G., et al., 2012. Statistical adaptation of ALADIN RCM outputs over the French Alps - application to future climate and snow cover. Cryosphere 6, 785–805. https://doi.org/10.5194/tc-6-785-2012.
Salerno, F., Guyennon, N., Thakuri, S., et al., 2015. Weak precipitation, warm winters and springs impact glaciers of south slopes of Mt. Everest (central Himalaya) in the last 2 decades (1994–2013). Cryosphere 9 (3), 1229–1247. https://doi.org/10.5194/tc-9-1229-2015.
Schattan, P., Baroni, G., Oswald, S.E., et al., 2017. Continuous monitoring of snowpack dynamics in alpine terrain by aboveground neutron sensing. Water Resour. Res. 53 (5), 3615–3634. https://doi.org/10.1002/2016WR020234.
Schmidli, J., Schmutz, C., Frei, C., et al., 2002. Mesoscale precipitation variability in the region of the European Alps during the 20th century. Int. J. Climatol. 22, 1049–1074. https://doi.org/10.1002/joc.769.
Schmucki, E., Marty, C., Fierz, C., et al., 2015. Simulations of 21st century snow response to climate change in Switzerland from a set of RCMs. Int. J. Climatol. 35, 3262–3273. https://doi.org/10.1002/joc.4205.
Schöber, J., Achleitner, S., Bellinger, J., 2016. Analysis and modelling of snow bulk density in the Tyrolean Alps. Hydrol. Res. 47 (2), 419–441. https://doi.org/10.2166/nh.2015.132.
Serquet, G., Marty, C., Dulex, J.-P., et al., 2011. Seasonal trends and temperature dependence of the snowfall/precipitation-day ratio in Switzerland. Geophys. Res. Lett. 38, 14–18. https://doi.org/10.1029/2011GL046976.
Smyth, E.J., Raleigh, M.S., Small, E.E., 2019. Particle Filter Data Assimilation of Monthly Snow Depth Observations Improves Estimation of Snow Density and SWE. Water Resour. Res. 55 (2), 1296–1311. https://doi.org/10.1029/2018WR023400.
Staudinger, M., Stahl, K., Seibert, J., 2014. A drought index accounting for snow. Water Resour. Res. 50, 7861–7872. https://doi.org/10.1002/2013WR015143.
Steger, C., Kotlarski, S., Jonas, T., et al., 2013. Alpine snow cover in a changing climate: a regional climate model perspective. Clim. Dynam. 41, 735–754. https://doi.org/10.1007/s00382-012-1545-3.
Steiner, L., Meindl, M., Fierz, C., et al., 2018. An assessment of sub-snow GPS for quantification of snow water equivalent. Cryosphere 12 (10), 3161–3175. https://doi.org/10.5194/tc-12-3161-2018.
Sturm, M., Taras, B., Liston, G.E., et al., 2010. Estimating snow water equivalent using snow depth data and climate classes. J. Hydrometeorol. 11 (6), 1380–1394. https://doi.org/10.1175/2010JHM1202.1.
Terzago, S., Fratianni, S., Cremonini, R., 2013. Winter precipitation in Western Italian Alps (1926–2010). Meteorol. Atmos. Phys. 119, 125–136. https://doi.org/10.1007/s00703-012-0231-7.
Thakur, B., Kalra, A., Lakshmi, V., et al., 2020. Linkage between ENSO phases and western US snow water equivalent. Atmos. Res. 236, 104827 https://doi.org/10.1016/j.atmosres.2019.104827.
Torrence, C., Compo, G.B., 1998. A practical guide to wavelet analysis. Bull. Am. Meteorol. Soc. 79 (1), 61–78. https://doi.org/10.1175/1520-0477(1998)079<0061:APGTWA>2.0.CO;2.
Torrence, C., Webster, P.J., 1999. The annual cycle of persistence in the El Niño/Southern Oscillation. Quarterly J. Royal Meteorol. Soc. 124, 1985–2004. https://doi.org/10.1002/qj.49712455010.
Valt, M., Cianfarra, P., 2010. Recent snow cover variability in the Italian Alps. Cold Reg. Sci. Technol. 64, 146–157. https://doi.org/10.1016/j.coldregions.2010.08.008.
Valt, M., Chiambretti, I., Dellavedova, P., 2012. YETI - a software to service the avalanche forecaster: Proceedings of advances in Avalanche forecasting. In: Richnavsky, J., Biskupic, M., Kyzek, F. (Eds.), Section 2 New Approaches and Tools for Avalanche Forecasting. Podbanské, Slovakia, pp. 38–43.
Valt, M., 2019. Criticità nelle misure per la stima dello SWE. IV Interconfronto SWE - Val di Susa 19–20 marzo 2018.
Vionnet, V., Fortin, V., Gaborit, E., et al., 2020. Assessing the factors governing the ability to predict late-spring flooding in cold-region mountain basins. Hydrol. Earth Syst. Sci. 24, 2141–2165. https://doi.org/10.5194/hess-24-2141-2020.

Winkler, M., Schellander, H., Gruber, S., 2021. Snow water equivalents exclusively from snow depths and their temporal changes: the ΔSNOW model. Hydrol. Earth Syst. Sci. 25, 1165–1187. https://doi.org/10.5194/hess-25-1165-2021.

World Meteorological Organization, 2012. Standardized Precipitation Index User Guide (M. Svoboda, M. Hayes and D. Wood). (WMO-No. 1090), Geneva.

Zampieri, M., Scoccimarro, E., Gualdi, S., 2013. Atlantic influence on spring snowfall over the Alps in the past 150 years. Environ. Res. Lett. 8, 034026 https://doi.org/10.1088/1748-9326/8/3/034026.

Zhang, B., Xia, Y., Huning, L.S., 2019. A framework for global multicategory and multiscalar drought characterization accounting for snow processes. Water Resour. Res. 55, 9258–9278. https://doi.org/10.1029/2019WR025529.